CCFE
CULHAM CENTRE FOR FUSION ENERGY

UK Atomic Energy Authority

UKAEA-CCFE-CP(23)19

M. VALOVIČ, Y. BARANOV, A. BOBOC, J. BUCHANAN, J. CITRIN, E. DELABIE, L. GARZOTTI, C. GIROUD, R. MCKEAN, E. LERCHE, E. DE LA LUNA, V. KIPTILY, F. KÖCHL, M. MARIN, S. MENMUIR, C. VON THUN, G. TVALASHVILI AND THE JET CONTRIBUTORS

CONTROL OF H/D ISOTOPE MIX BY PERIPHERAL PELLETS IN H-MODE PLASMA IN JET

CONTROL OF H/D ISOTOPE MIX BY PERIPHERAL PELLETS IN H-MODE PLASMA IN JET

M. VALOVIČ, Y. BARANOV, A. BOBOC, J. BUCHANAN, J. CITRIN, E. DELABIE, L. GARZOTTI, C. GIROUD, R. MCKEAN, E. LERCHE, E. DE LA LUNA, V. KIPTILY, F. KÖCHL, M. MARIN, S. MENMUIR, C. VON THUN, G. TVALASHVILI AND THE JET CONTRIBUTORS

This paper has been submitted to
28th IAEA Fusion Energy Conference, Nice, France, 10-15th May 2021

CONTROL OF H/D ISOTOPE MIX BY PERIPHERAL PELLETS IN H-MODE PLASMA IN JET

M. VALOVIČ[1], Y. BARANOV[1], A. BOBOC[1], J. BUCHANAN[1], J. CITRIN[2], E. DELABIE[3], L. GARZOTTI[1], C. GIROUD[1], R. MCKEAN[1], E. LERCHE[1,5], E. DE LA LUNA[4], V. KIPTILY[1], F. KÖCHL[1,6], M. MARIN[2], S. MENMUIR[1], C. VON THUN[7], G. TVALASHVILI[1] AND THE JET CONTRIBUTORS*

EUROfusion Consortium, JET, Culham Science Centre, Abingdon, OX14 3DB, UK
[1]CCFE, Culham Science Centre, Abingdon, OX14 3DB, UK
[2]DIFFER P.O. Box 6336, 5600 HH Eindhoven, The Netherlands
[3]Oak Ridge National Laboratory, Oak Ridge, Tennessee, United States of America
[4]Laboratorio Nacional de Fusión, Ciemat, 28040 Madrid, Spain
[5]LPP-ERM/KMS, Association EUROFUSION-Belgian State, TEC partner, Brussels, Belgium
[6]Fusion@ÖAW, Atominstitut, TU Wien, Stadionallee 2, A-1020 Vienna, Austria
[7]Institute of Plasma Physics and Laser Microfusion, Hery 23, 01-497 Warsaw, Poland

*See the author list of 'Overview of JET results for optimising ITER operation' by J. Mailloux et al to be published in Nuclear Fusion Special issue: Overview and Summary Papers from the 28th Fusion Energy Conference (Nice, France, 10-15 May 2021)

E-mail: martin.valovic@ukaea.uk

Abstract

Control of plasma H:D isotope mix using solely shallow pellets (in H or D) was demonstrated in recent experiments, attaining ~50%:50% ratio. The isotope mix propagates from the edge to the core on the confinement timescale. Isotope dependence of energy confinement is within error bar to scaling laws. A dataset is collected for different pellet sizes, isotope content and plasma current, and including for the first time pellets with ITER-like ablation and relative pellet size. Data indicate high ablation efficiency for pellets with ablation depth r/a<0.95, but falling sharply for shallower pellet deposition.

1. INTRODUCTION

In ITER the density of deuterium and tritium will be controlled by injection of cryogenic pellets, with D and T isotopes separately (at least some) to allow active isotope ratio control. Due to technical limitations pellet velocity is limited to 300m/s. This combined with high pedestal temperatures results in pellet ablation depth about the same as the width of edge transport barrier. For deeper penetration one has to invoke curvature drift and inward particle transport. Another parameter governing the ITER pellet fuelling is rather small relative size of the pellets which is difficult to match in medium size machines.

This paper present unique pellet fuelling dataset from JET addressing aforementioned issues. Two sets of experiments are presented. Firstly the hydrogen-deuterium mix is controlled with mono-isotopic pellets, although only one injector is used at a time and second isotope is provided by gas and beams. Second experiment is devoted to pellet ablation for both isotopes. Here for the first time pellets with ITER like peripheral ablation and relative size are injected into high current high power JET plasmas.

2. INJECTION OF DEUTERIUM PELLETS INTO HYDROGEN PLASMA

This experiment was performed with plasma current $I_p = 1.4MA$ and toroidal field on geometric axis $B_T = 1.7\ T$. The divertor was in corner configuration for both inner and outer leg. Plasma fuelling was provided by hydrogen gas with a rate of $\Phi_{H2,gas} = 6.7 \times 10^{21}\ at/s$, which was reduced to $5.2 \times 10^{21}\ at/s$ during the pellet phase (see figure 1c). Plasma was heated by hydrogen beams of $P_{NB} = 6.3MW$. In addition, RF heating at second harmonic hydrogen resonance is used ($\omega = 2\omega_{cH}$, 51MHz) with power of $P_{RF} = 3.3MW$

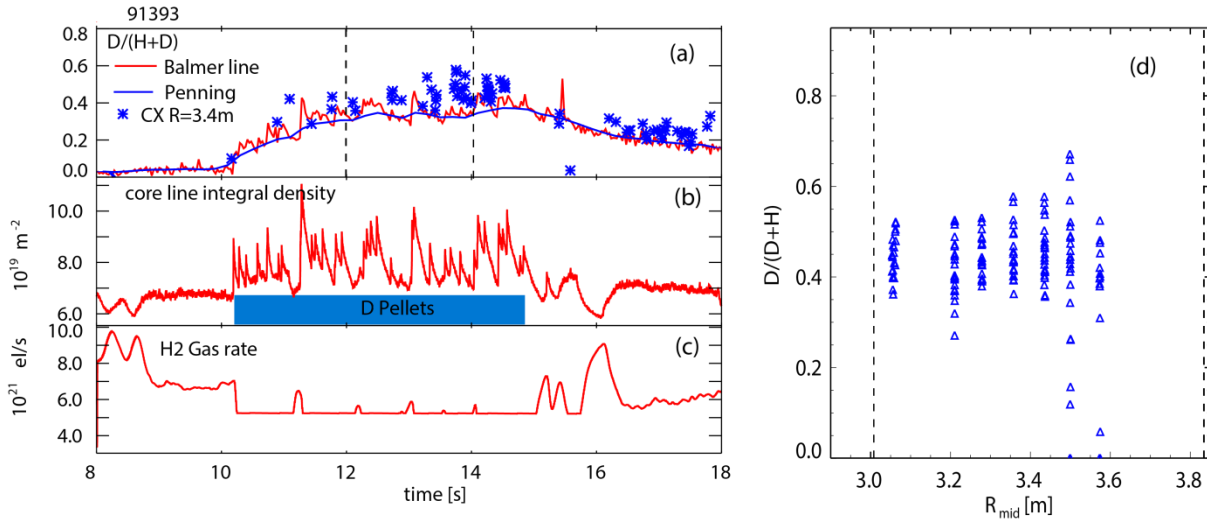

FIG. 1. *Temporal evolution of relevant parameters during the isotope control experiment. Traces from the top to the bottom: (a) isotope mix ratio from: Balmer line spectroscopy - red line, Penning pressure gauges in divertor - blue line, CX spectroscopy at R=3.43m (normalised minor radius r/a=0.27) – blue symbols, (b) core line integrated density $n_e L$, (c) hydrogen gas puff rate, (d) isotope mix ratio profile from CX spectroscopy for time interval shown by vertical lines on panel (a), vertical lines in panel (d) represent magnetic axis and separatrix respectively. For given radius different data points represent different times (Reproduced courtesy of IAEA. Figure from [1]. © 2019 EURATOM).*

so that the total auxiliary heating power during flattop is $P_{aux} = 9.6MW$. For full details see [1].

After stationary hydrogen H-mode is established, fuelling by ~20mm^3 deuterium pellets ($N_{pel} = 8.5 \times 10^{20}\ at$) from the high field side is applied (see figure 1). The reduction from nominal pellet size of 40mm^3 was possible by "double cut" method. With pellet rate of 9.7 Hz the fuelling rate is $\Phi_{pel} = 8.2 \times 10^{21}\ at/s$. The pellet velocity is$\sim 90\mathrm{m/s}$.

During injection of deuterium pellets into hydrogen plasma the isotope mix ratio was measured by four independent methods: Balmer-alpha spectroscopy, Penning gauges, charge exchange spectroscopy in the plasma core, and from neutron rate. The first three methods are shown in figure 1a. It is seen that all three methods show that at the flat top the isotope mix ratio $n_D/(n_H + n_D) = 0.45$ was reached, close to the target of 50%:50%.

The fourth method for evaluating isotope mix is from neutrons Figure 2a shows that application of deuterium pellets causes an increase of neutron rate from virtually zero to the flat top value. Assuming that all neutrons are the result of a thermal DD reaction and knowing the density and temperature profiles one can convert the neutron rate into the isotope mix ratio in the centre. The problem is the discrete nature of pellet fuelling which makes the plasma density transient at all times. To include this element into the analysis, we calculated the plasma density by a model while keeping the temperature fixed from the measurement. Figures 2c, 2e and 2f document how the experimental ion temperature was imported into the simulation and quality of the assumption $T_i = T_e$.

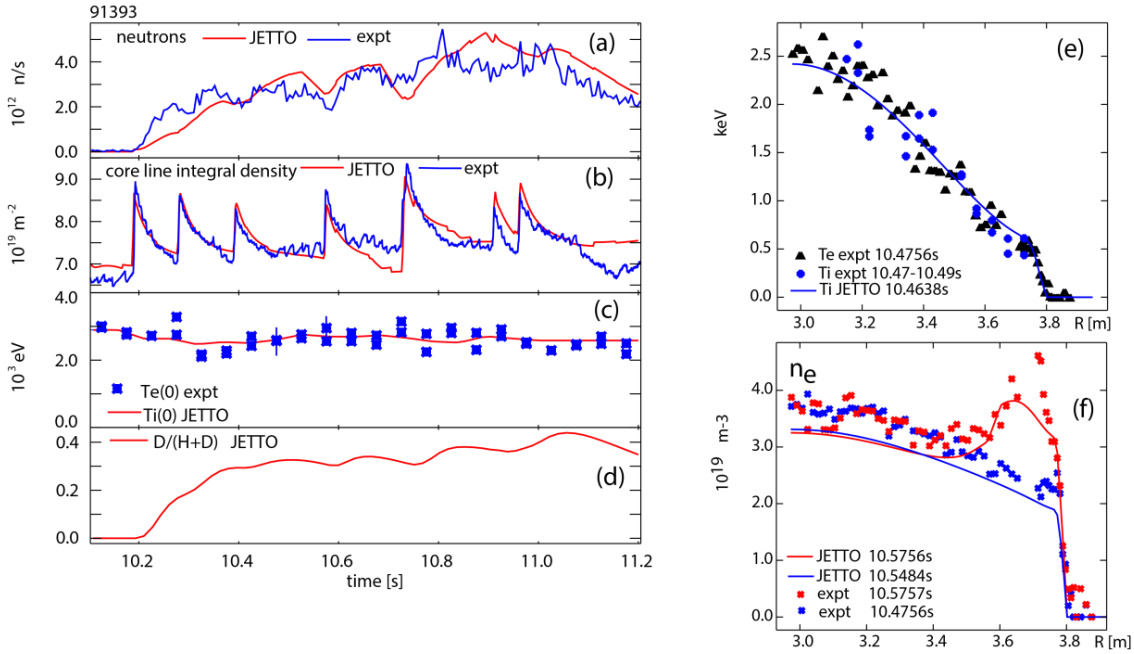

FIG. 2. *Isotope mix control by pellets. (a) total neutron rate* $R_{DD,th}$*, (b) core line integrated density* $n_e L$ *with error bar of* $5\times 10^{17} m^{-2}$*, (c) central electron temperature from Thomson scattering (blue + symbols) and central ion temperature as imported into JETTO (red line), (d) calculated central isotope mix ratio* $n_D/(n_H + n_D)$ *from neutron rate, (e) electron and ion temperatures and (f) electron density profiles before and after 4th pellet. In panels (e) and (f) electron density and temperature is measured by Thomson scattering. (Reproduced courtesy of IAEA. Figure from [1]. © 2019 EURATOM).*

The model evolves independently hydrogen and deuterium densities as a response to particle sources and particle transport. The simulation was done by JINTRAC code suite [2]. The particle sources include beams, pellets and neutrals, and are calculated by PENCIL, HPI2 and FRANTIC codes respectively. The boundary condition for FRANTIC is set by neutral hydrogen flux at separatrix $\Phi_0 = 2.7 \times 10^{21} at/s$. For plasma core the particle diffusivity is used as $\mathrm{D} = C_D \times \chi_{BgB}$, where χ_{BgB} is the geometric average of electron and ion Bohm/gyro-Bohm heat diffusivities [2] and the C_D multiplier is set the same for hydrogen and deuterium. In addition, modest inward anomalous pinch is included as: $\mathrm{v/D} = -C_V \mathrm{r}/a^2$. At the plasma edge the particle transport is modelled by "continuous ELM model" [2] in which the particle diffusivity inside edge transport barrier is enhanced when the pressure gradient exceeds a critical value: $\alpha > \alpha_{crit}$. In addition it was necessary to add transient post pellet outward convection in the form of $\mathrm{v} = v_0 \times exp\{-(t - t_{pel})/\tau + (r/a - 1)/\Delta\}$ where v_0 is the amplitude of outward convection, τ is the duration of the enhanced post pellet convection and Δ is the normalised radial depth of the zone of the enhanced convection.

Figure 2 shows the result of the simulation with the following parameters, $C_D = 4.5$, $C_V = 0.4$, $v_0 = 7m/s$, $\tau = 50\mathrm{ms}$, $\Delta = 0.25$, and using the same values for hydrogen and deuterium. These parameters are derived iteratively until good agreement in neutron rate and density is found. It is seen that the calculated isotope mix ratio in the core is comparable with the edge values.

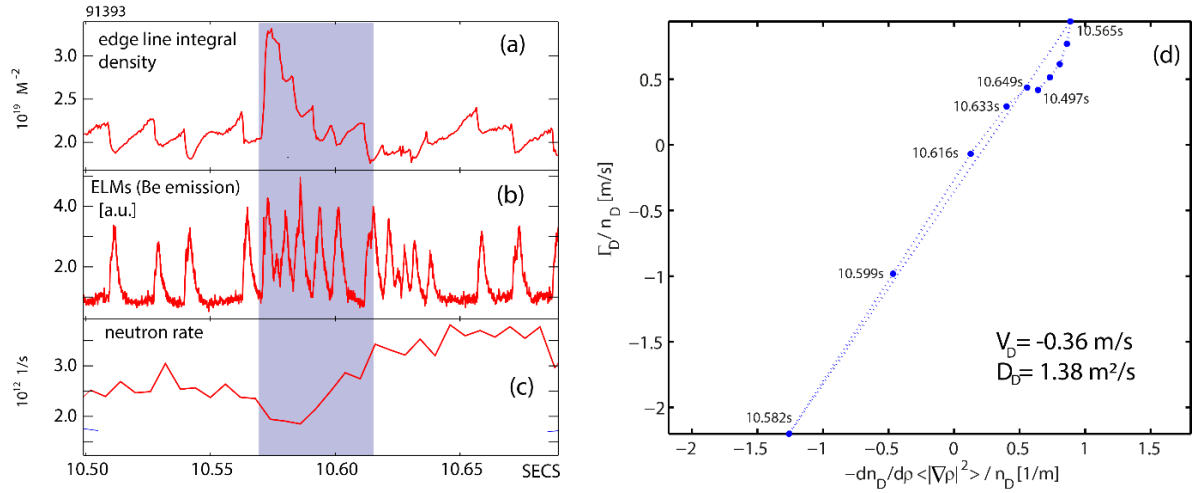

FIG. 3. Detail of transient around the 4th pellet. (a) edge line integral density, (b) ELMs signals, (c) neutron rate. Shaded area in panels (a)-(c) approximately represents the interval with inverted density gradient. (d) plot of the normalised particle flux Γ_D/n_D *versus normalised density gradient* $dn_D/dr/n_D$ *at r/a = 0.5. corresponding time labels are shown. (Reproduced courtesy of IAEA. Figure from [1]. © 2019 EURATOM).*

When pellet is injected into plasma it creates transiently a zone of reversed gradient of deuterium density. As a consequence, the deuterium ion particle flux reverses from outwards to inwards. This situation is transient and for single pellet is detailed in figure 3. When evaluated during post pellet phase at r/a=0.5 the deuterium particle diffusivity is $D_D = 1.38m^2/s$ as seen in figure 3d. In normalised units the deuterium diffusivity is $D_D/\chi_{eff} = 0.41$. Here $\chi_{eff} = q/(n_e\nabla T_e + n_i\nabla T_i) = 3.3m^2/s$ is the experimental effective single fluid heat diffusivity averaged over the pellet cycle and q is the total heat flux density. It has to be noted that pellets can also modify the temperature profile due to the local cooling and this can change heat diffusivity itself. In our case the heat diffusivity changes are within $\chi_{eff} = 2.4 - 3.8m^2/s$.

The neutron rate after the first pellet in figure 1 increases faster than predicted by JETTO Bohm-gyro Bohm model. If enhancement of neutron rate by nuclear knock-on effect due to RF heating [1] is insignificant then penetration of deuterium to the plasma core is faster at the beginning of pellet train compared to the later pellet fuelling phase. The gyro-kinetic simulations show that indeed in ion temperature gradient regime the diffusivities for both ion species are higher than the electron diffusivity $D_H \sim D_D > D_e$ [3, 4, 5]. This could explain the fast propagation of isotope mix from the edge to the core even with similar (but not equal) diffusivities for hydrogen isotopes. In other words our assumption of similar particle transport coefficients for the different isotopes is not in contradiction to a possible 'isotope effect', whereby transport may be significantly modified when transitioning from a hydrogen dominated to a deuterium dominated plasma. The detailed gyro-kinetic modelling of core particle transport under our condition of isotope mixing by pellets is subject of separate paper [6].

3. INJECTION OF HYDROGEN PELLETS INTO DEUTERIUM PLASMA

In second experiment hydrogen pellets were injected into plasma with deuterium gas and beams. The plasma current, magnetic field and heating power is the same as in previously described plasma. Pellets nominal size was 40mm^3, rate 10Hz and velocity 233m/s. Figure 4 shows that in this shot 97100 the edge isotope mix ratio starts at predominantly deuterium level. Application of hydrogen pellets gradually reduces the H/D isotope mix close to half and half value. The duration of this transient is about 2s.

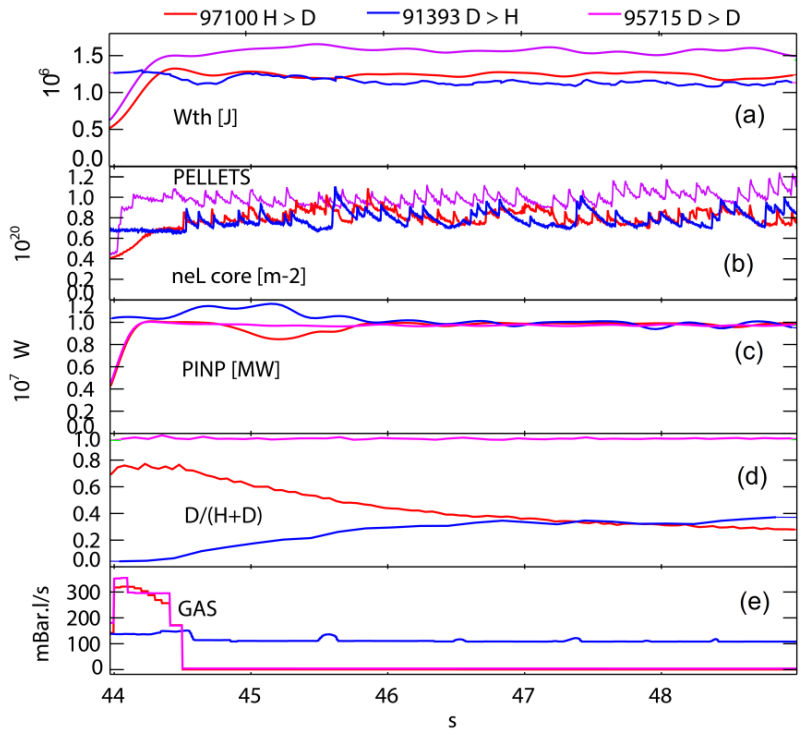

FIG. 4. Comparison of pellet fuelling using different combinations of hydrogen isotopes. Shot 91393 (blue lines): H gas, H NBI, D pellets. Shot 97100 (red lines): D gas, D NBI, H pellets. Shot 95715 (pink lines): D gas, D NBI, D pellets. Panel (a) thermal energy content from diamagnetic loop, (b) central line integrated density, (c) input power, (d) isotope ratio $n_D/(n_H + n_D)$ from divertor spectroscopy, (e) gas injection waveforms. Time base is shifted for shot 91393.

For comparison figure 4 shows also the traces for shot with deuterium pellets and hydrogen plasma 91393. Both shots have the same transient time to reach the half and half mix. The shot 97100 with H pellets has slightly higher (15%) thermal energy content W_{th} compared to the shot 91393 with D pellets. This difference is the same in electron energy and EFIT energy contents (W_{th} from diamagnetic loop and EFIT agree within 7%). These similarities indicate that close to half and half mix the isotope dependence of pellet fuelling is small.

For completeness figure 4 shows also traces for purely deuterium case, shot 95715. This plasma has higher W_{th} by a factor of ~1.2 compared to mixed isotope cases indicating higher energy confinement. Such increase is within the error bar what is expected from scaling from combined effect of higher density (~20%) and isotope dependence: $\tau_E \propto n^{0.41} M^{0.19-0.4} \propto 1.2^{0.41}(2/1.4)^{0.19\div 0.4} = 1.15\div 1.24$. Here the density exponent is taken from IPB98y2 scaling and two values of mass exponents come from IPB98y2 and from [6] respectively.

The isotope mix ratio in figure 4 is measured in the divertor and with slow frame rate - about the same as the pellet rate. In order to determine the isotope mix ratio in the core and with higher temporal resolution we used the modelling similar to that in section 2. The only difference is the use of ASCOT code for neutron rate due to dominant beam – thermal component. As in section 2 the temperature is taken from measurement. Figure 5 shows the result of such analysis during first 6 pellets. The plasma electron density is reproduced by the particle transport model. The neutron rate is also reproduced well during the first pellets but later the model gradually departs from experiment, namely it underestimates the hydrogen density in the core.

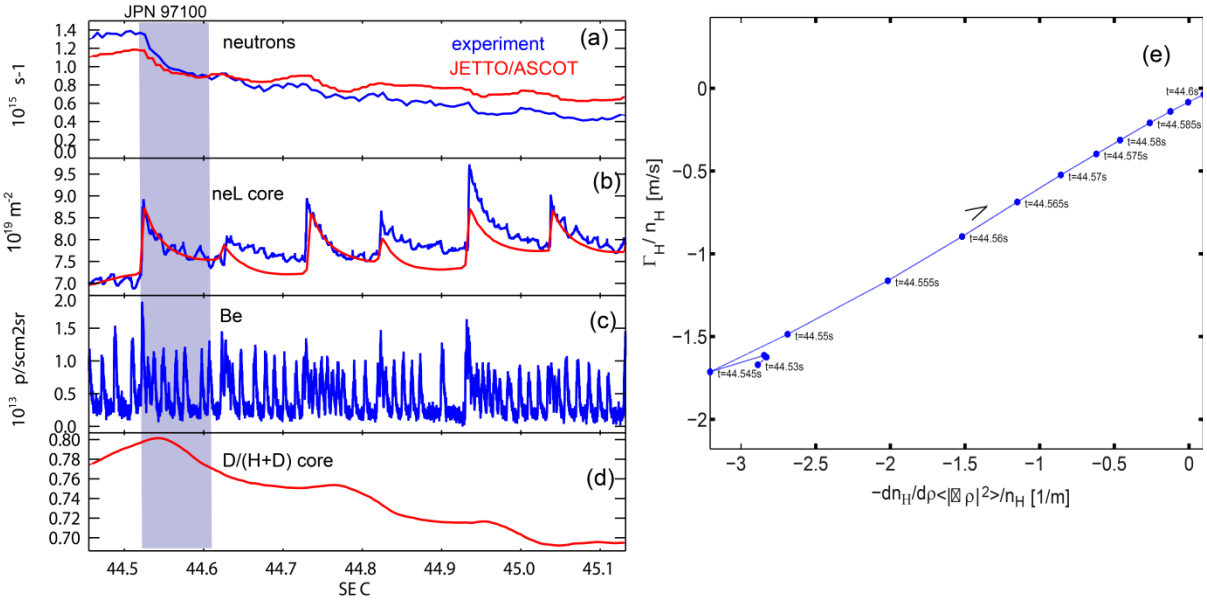

FIG. 5. Isotope mix control by hydrogen pellets, experiment and modelling. (a) total neutron rate (b) line averaged density n_{eL}, (c) Be emission as ELM indicator, (d) central isotope mix ratio $n_D/(n_H + n_D)$ from modelling, (e) hydrogen ion flux density v.s. density gradient during the first pellet cycle (gray area on left panel) - both quantities are normalised and taken at r/a=0.5.

Figure 5 shows the evolution of hydrogen flux and gradient of ion hydrogen density after the first pellet at r/a=0.5. The slope of the trajectory gives the hydrogen diffusivity of $D_H = 0.53m^2/s$. The heat diffusivity averaged over interval after the first pellet is $\chi_{eff} = 2.7\, m^2/s$ so that $D_H/\chi_{eff} = 0.20$. This value is factor of two smaller than in case of deuterium pellets injected into hydrogen plasma. Nevertheless in both cases the propagation of isotope mix from the edge to the core for a single pellet takes 60-70ms which is about 1/2 of energy confinement time. Note that this time reflects not only inward particle transport but also outward pellet particle loss due to ELMs.

4. PELLET DEPOSITION EFFICIENCY

One of the key parameters controlling the pellet fuelling is the pellet ablation depth, or the innermost normalised radius reached by a pellet, r/a . This can be calculated from the fast interferometer and ablation light signals. Figures 6a and 6b show that the duration of pellet ablation coincides well with the duration of pellet deposition determined from interferometer signal Δt_{dep}. The pellet deposition radius is then calculated as $r/a = 1 - \gamma v_{pel}\, \Delta t_{dep}\, /(ak)$, where v_{pel} is the pellet velocity, a is the plasma minor radius, k is the plasma elongation and $\gamma = 0.68$ is the geometric factor. In rare cases when the time of Thomson scattering measurement is close to the end of pellet deposition one can compare the ablation depth with post pellet density profile. As seen in figure 6c the pellet deposition determined from duration of ablation approximately coincides to the maximum of density perturbation which is consistent with grad–B drift being comparable with ablation depth.

Finally note that the abrupt change of slope of interferometer signal (figure 6b) at the end of ablation process is imposing interesting constraint on pellet ablation model. Namely one can calculate ablation rate towards the end of pellet lifetime and compare with theory. Such analysis is outside the scope of present paper.

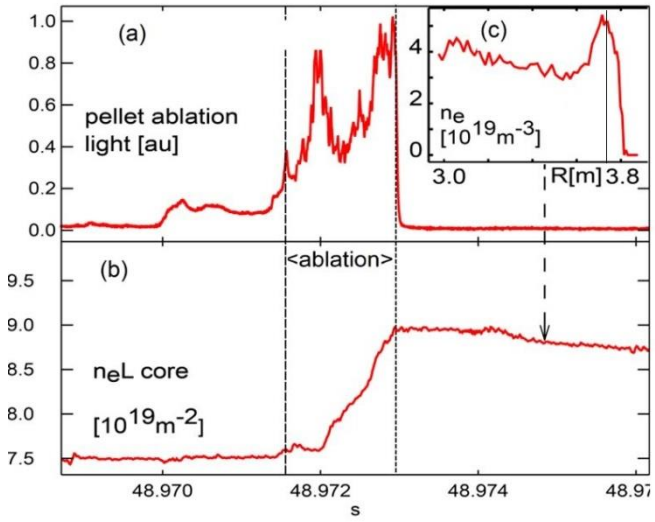

FIG. 6. Temporal resolution of pellet ablation. (a) pellet ablation visible light, (b) high resolution interferometer signal, (c) density profile from Thomson scattering at time shown by arrow in panel (b). The vertical line in panel (c) shows the radius calculated from the duration of the ablation.

Figure 7a shows the pellet ablation depth for both nominal pellet sizes, isotope contents and plasma currents. The vertical axis shows the relative plasma density perturbation by pellet during ablation calculated from core interferometer signal as $\Delta(n_eL)_{dep}/(n_eL)$ where $\Delta(n_eL)_{dep}$ is the change of line integral across the ablation interval. This quantity includes also prompt losses of plasma material, mainly due ELMs triggered by pellets. It is seen that pellet deposition clearly correlates with relative density perturbation by pellet, i.e. deeper pellets cause larger perturbation. In addition JET dataset populate the region predicted for ITER, which is difficult to achieve on smaller tokamaks.

Figure 7b shows the efficiency of pellet deposition as a function of pellet ablation depth r/a. The efficiency is calculated as $\Delta N_{dep}/N_{pel,\mu}$. Here ΔN_{dep} is the number of pellet deposited electrons, including prompt losses, estimated from interferometer signal $\Delta(n_eL)_{dep}$ and $N_{pel,\mu}$ is the number of pellet atoms measured by microwave cavity (No5) close to the end of flight line. The data indicate high injection efficiency for ablation depth r/a<0.95 and falling sharply for shallower pellets. The low efficiency for shallower pellets is correlated with prompt ELMs. No difference between hydrogen and deuterium pellets is observed. The exception is the lower efficiency for large hydrogen pellets which could be due to losses in the last part of the flight line.

Finally note that the JET data set covers the predicted deposition of fuelling pellets on ITER [8] though more data and analysis is needed to gain confidence.

5. CONCLUSIONS

We have demonstrated control of H:D isotope mix in the plasma core when one isotope was delivered solely by shallow pellets. Both H and D pellets were used and the H:D isotope mix reached close 50% :50% ratio. Isotope mix propagates to the core on confinement timescale, in agreement with quasilinear theory [5]. Isotope ion diffusivities are larger than the electron diffusivity what is favourable for isotope mix control.

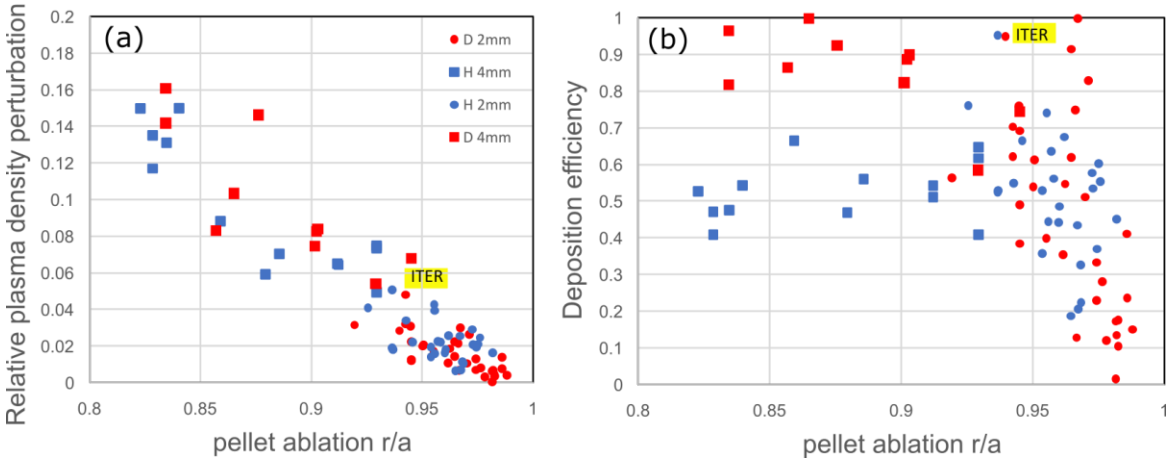

FIG. 7. (a) relative perturbation of plasma density by pellet and (b) pellet deposition efficiency, both as a function of ablation depth. Each data point represents one pellet. All quantities are calculated from fast interferometer signal as shows in figure 6.

Simulations also reveal the importance of particle transport in outer part of the plasma. In particular core isotope mix ratio is sensitive to pellet particle loss in pellet deposition zone. These losses are attributed to ELMs acting in plasma periphery and are added in models as mixed conduction and convection.

Pellet deposition efficiency was measured for different pellets sizes, pellet isotope content and plasma current. Data show high efficiency for pellets with ablation depth r/a<0.95, but falling sharply for shallower pellets. This dataset for the first time covers the pellets with ITER like ablation depth and relative pellet size. No difference on pellet isotope content is observed. The exception are large hydrogen pellets showing lower efficiency which is not understood so far.

Finally it has to be noted that the deposition efficiency in figure 7 is different from the overall pellet fuelling efficiency - which is the convolution of flight line losses, deposition efficiency and post-pellet losses.

ACKNOWLEDGEMENTS.

This work was carried out within the framework of the EUROfusion Consortium and received funding from the Euratom research and training programme 2014–2018 and 2018-2020 under grant agreement No. 633053 and from the RCUK Energy Programme grant No. EP/P012450/1. The views and opinions expressed herein do not necessarily reflect those of the European Commission. This scientific work was partly supported by the Polish Ministry of Science and Higher Education within the framework of the scientific financial resources in the year 2020 allocated for the realization of the international co-financed project No 5118/H2020/EURATOM/2020/2.

REFERENCES

[1] VALOVIČ M et al Nucl Fusion 59 (2019)106047
[2] ROMANELLI M., et al Plasma and Fusion Research 9 (2014) 3403023
[3] BOURDELLE C. et al Nucl. Fusion 58 (2018) 076028
[4] MASLOV M. et al Nucl. Fusion 58 (2018) 076022
[5] MARIN M. et al Nucl. Fusion 61 (2021) 036042
[6] MARIN M. et al this conference
[7] MAGGI C. et al Plasma Physics and Controlled Fusion 60 (2018) 014045
[8] POLEVOI A R et al Nucl. Fusion 58 (2018) 056020